Effect of pipernonaline from Piper retrofractum on memory disorder in mice and neurite outgrowth activity of PC12 cells

Runa Fujimoto
Gifu University
Yuzuki Irie
Gifu University
Tohru Mitsunaga
Gifu University
Kosei Yamauchi
yamauchi.kosei.p2@f.gifu-u.ac.jp

Gifu University

Research Article

Keywords: Piper retrofractum, PC12 cell, memory disorder, structure-activity relationships

Posted Date: June 19th, 2026

DOI: https://doi.org/10.21203/rs.3.rs-9992365/v1

Additional Declarations: No competing interests reported.

Abstract

In this study, we discovered compounds comprising a piperidine skeleton in Piper retrofractum; the compounds exhibit PC12 dendrite elongation activity. Furthermore, we examined the structure-activity relationship by comparing the activities of the isolated compounds 1, 3–7. Among the isolated compounds, two alkaloids (6 and 7) displayed significant neurite outgrowth (NOG) effects in the presence of 5 ng/mL nerve growth factor (NGF) in a dose-dependent manner. Comparison of the activity of 3 (Pipercide; 1.8% NOG positive at 100 μM), 6 (Dehydropipernonaline; 21.1% NOG positive at 100 μM), and 7 (Pipernonaline; 24.3% NOG positive at 100 μM) demonstrated that the piperidine skeleton is key to NOG activity. Furthermore, the carbon chain length and number of double bonds influence NOG activity. Moreover, the Barnes maze test showed that oral administration of compound 7 in mice improved memory disorders induced by scopolamine and corticosterone. These results provide extremely valuable foundational knowledge for elucidating the cognitive function-improving effects of P. retrofractum, a food spice.

Introduction

As the global population ages, the incidence of dementia continues to rise. Japan is facing a super-aging society, and improving the treatment of dementia is an urgent challenge. The number of patients with dementia worldwide was approximately 50 million in 2020[1]. Furthermore, the number of patients is estimated to reach 152 million by 2050[1]. Alzheimer's disease (AD) is the most common type of dementia, particularly among patients aged > 65 years old. AD is a progressive neurodegenerative disease characterized by memory loss and cognitive impairment [2]. The cholinergic hypothesis, which posits that a decrease in the amount of the neurotransmitter acetylcholine (Ach) in the brain causes Alzheimer's disease (AD), is the prevailing theory. This hypothesis suggests that dysfunction of Ach neurons leads to cognitive decline. In the treatment of AD, acetylcholinesterase (AchE) inhibitors have been studied for many years, and currently, drugs such as donepezil, tacrine, and galantamine are primarily used.

NGF, the first neurotrophic factor, is a homodimer of non-covalently linked polypeptide chains of approximately 120 amino acid residues. NGF is present in both the central and peripheral nervous systems, particularly promoting the survival and differentiation of cholinergic neurons in the central nervous system [3]. NGF also plays a crucial role in the differentiation of neural stem cells [2]. Therefore, the neurogenesis effects of neurotrophic factors such as NGF are expected to be applicable to the treatment of dementia. However, owing to the macromolecule, NGF cannot cross through the blood-brain barrier (BBB)[3]. In addition, the direct administration of NGF to the brain causes side effects such as pain[3]. Therefore, Therefore, the use of small molecule compounds exhibiting NGF-like activity is clinically promising.

Several reports have investigated the link between daily dietary habits and various diseases, including lifestyle-related illnesses [4]. In particular, the incidence of dementia per age group is reportedly lower in

areas where spices are frequently used. Thus, there is growing interest in the effects of spices on cognitive function. Capsaicin, known as the main pungent component of chili peppers, cross the blood-brain barrier, suppresses Aβ production in the brain of AD model mice, and reduces cognitive dysfunction[5]. Further, capsaicin binds to transient receptor potential vanilloid1 (TRPV1), which is expressed in sensory neurons, hippocampal pyramidal neurons, dentate gyrus, hypothalamus, substantia nigra, and the cerebral cortex[6]. TRPV1 plays an important role in the regulation of synaptic plasticity[5]. Activation of TRPV1 triggers long-term depression (LTD) of excitatory synapses in hippocampal interneurons and is involved in memory formation[7]. Moreover, the activation of TRPV1 induces intracellular Ca^{2+} influx, activates calmodulin and calmodulin-dependent kinase (CaMK), and promotes CREB phosphorylation, which in turn promotes neuronal differentiation[8]. We expect that the search for compounds with NGF-like effects and the elucidation of their mechanisms will contribute to the prevention and early treatment of Alzheimer's disease (AD).

Spices and herbs have been used since ancient times as preservatives and flavoring agents, and in religious rituals. Spices were highly valued in Europe during the Middle Ages. Additionally, spices are used as herbal medicines in their country of origin and have a long history of being used for the treatment of diseases[9]. Differences in the prevalence of various diseases among countries and regions have been reported, suggesting a relationship between diet and disease. The use of different spices is unique to each region. Interest in the health benefits, such as the disease-preventive or curative effects of spices and herbs, is growing[10].

Piper retrofractum, a member of the Piperaceae family, is widely distributed in Southeast Asia, including Indonesia, Sri Lanka, Vietnam, and the Philippines. *Piper* genus fruits are known as hihatsu in Japan and have been used as a spice because of their pungent flavor[11]. *Piper* plants have also been used in herbal medicines for menstrual cramps, sleep disorders, gastrointestinal pain, and arthritis[11]. The pungency of *Piper* plants is mainly caused by alkaloidal compounds such as piperine. Many alkaloidal compounds have been isolated from *Piper* plants[12],[13],[14]. *P. retrofractum* has been reported to significantly induce neurite outgrowth in PC12 cells and improve anxiety and depression in AD model rats[15]. However, few studies have focused on the NOG effect, and the effective ingredients for memory improvement remain unknown. In this study, we aimed to discover the active compounds from *P. retrofractum* with clarifying the structure-activity relationships that displayed the most pronounced NOG-inducing effect and improved memory disorders in mice.

Results and Discussion

Fractionation of P.retrofractum 70%EtOH extracts

The yield of the *P.retrofractum* 70% ethanol extract obtained from the *P.retrofractum* dried fruit powder (2.4 kg) was 188 g. The yields obtained from the EtOH extract by sequential extraction with hexane, diethyl ether, EtOAc, and MeOH were 48.5, 43.3, 6.93, and 14.7 g, respectively. The major component (**1**) of the *P.retrofractum* 70% EtOH extract, which was detected at r.t. 26.6 min, was isolated by

crystallization of the ethyl acetate extract. To identify the active compounds in the *P.retrofractum* 70% EtOH extract, further fractionation was conducted. The active compounds were obtained from the hexane extract that showed the most significant NOG effect on PC12 cells. The hexane extract (17 g) was subjected to normal-phase silica gel column chromatography, and 13 fractions (HFr.1-13) were obtained (Fig. 1).

Compound **2** was isolated by crystallization of HFr.6. The Hr.11 fraction was subjected to preparative HPLC, and compounds **3** (24.3 mg) and **4** (51.7 mg) were isolated. To obtain the active compounds from *P.retrofractum* hexane extracts, HFr.13, which showed significant NOG, was further separated. HFr.13 (2.0 g) was subjected to normal-phase silica gel column chromatography to obtain 11 fractions (HFr.13 − 1–11). To isolate the major components of HFr.13, HFr.13 − 10 and HFr13-8 were separated by preparative HPLC to obtain **5** (30.1 mg) from HFr.13 − 10 and **6** (9.1 mg), and **7** (71.9 mg) were obtained from HFr.13 − 8 (Fig. 1). All isolated compounds were identified using NMR and MALDI-TOF-MS by comparison with the previous reports described in Section 2.6. 2D NMR correlations of each compound supported the identified structures (Fig. 2).

Evaluation of the neurite outgrowth (NOG) effects

In this study, we investigated the effects of *P.lomgum* fruit components on NOG in rat adrenal medulla-derived pheochromocytoma PC12 cells.

The percentages of NOG-positive cells in each soluble part are shown in Fig. 3(A, B), and photomicrographs of PC12 are shown in Fig. S1 and S2. The hexane and diethyl ether extracts displayed weak NOG in the absence of NGF (Fig. 3A). Figure 3B indicates that the 70% EtOH extract (100 μg/mL), hexane fraction (50 μg/mL), diethyl ether fraction (50 μg/mL), and ethyl acetate fraction (100 μg/mL) exhibited a NOG effect in contrast to the control under the condition with NGF (5 ng/mL). Among the soluble components, the hexane extract displayed the most significant effect on NOG. These results indicate that the low-polarity compounds in *P. retrofractum* contribute to NOG. The percentages of NOG-positive cells in each fraction separated from the hexane extract are shown in Fig. 3(C, D). HFr. 7, 8, 12, and 13 exhibit significant effects on NOG in the absence of NGF, as shown in Fig. 3C. Figure 3D shows that HFr. 7–13 stimulate NOG effect (50%–30% of positive cell rate) compared with the control in the presence of a 5 ng/mL NGF (less than 5% of positive cell rate). Thereafter, the fractions displaying activity were used to isolate the active compounds in the *P. retrofractum* extract.

The percentages of NOG-positive cells after treatment with the isolated compounds are shown in Fig. 4(A, B). Compounds **6** and **7** exhibited significant NOG (Fig. S2). As shown in Fig. <link rid="fig4">4</link>B, 3 and 4 display no significant effect on NOG, while a concentration of 100 μM of **6** and **7** increases the NOG in positive cells to 21.1% and 24.3%, respectively, in the presence of 5 ng/mL of NGF. These results suggest that the piperidine skeleton attached to a carbonyl group provided NOG activity (Fig. 6). Comparing the activities of **6** and **7**, a small number of double bonds between the C2 and C9 carbon chains increased the NOG activity (Fig. 5), suggesting that the flexibility of the carbon chain is

important for NOG activity. Furthermore, the longer carbon chain stimulated NOG activity by comparison with the activity of compound **5** (10.2% NOG positive at 100 μM with 5 ng/ml NGF) and **7** (Fig. 5, 6). These results indicate that the carbon chain length plays an important role in this activity.

PC12 cells were incubated for 72 h with (A)Extracts of 70% EtOH, Hexane, diethyl ether, EtOAc, and MeOH from *P. retrofractum* dried fruit, (B) Extracts of 70% EtOH, Hexane, diethyl ether, EtOAc, and MeOH from *P. retrofractum* dried fruit with NGF 5ng/ml. PC12 cells were incubated for 72 h with (C)HFr.1–13 from *P. retrofractum* hexane extract, (D) HFr.1–13 from *P. retrofractum* hexane extract with NGF 5ng/ml. Significance was analyzed using analysis of Dunnett's test by EZR ***P < 0.001, **P < 0.01 and *P < 0.05 against the control value.

PC12 cells were incubated for 72 h with (A)Compound **1**-**7** from *P. retrofractum* Hexane extract, (B)Compound **1**–**7** from *P. retrofractum* hexane extract with NGF 5ng/ml. Significance was analyzed using analysis of Dunnett's test by EZR ***P < 0.001, **P < 0.01 and *P < 0.05 n = 3

Activation of TRPV1 induces intracellular Ca^{2+} influx and promotes CREB phosphorylation, which in turn promotes neuronal differentiation[8]. The binding of capsaicin and piperine to TRPV1 has been reported by Dong et al. Capsaicin produces two specific hydrogen bonds via T551 and E571. Moreover, piperine interacts with TRPV1 via the T551 and T671 receptors[6]. The mode of interaction between piperine derivatives and TRPV1 remains unknown. However, these results suggest that longer and more flexible carbon chains may interact strongly with the binding pocket of TRPV1.

Studies of *P.lomgum* fruit extracts and isolated compounds in AD are limited, and their effects are still unclear, although reports state that *P.lomgum* fruit extracts improve anxiety and depression in AD model rats. PC12 cells were first isolated from rat adrenal medullary pheochromocytoma by Greene and Tischler in 1976; the cells stopped the proliferation and elongation of neurites in the presence of NGF[16]. Therefore, PC12 cells have been widely used as neural model cells. NGF binds to the transmembrane TrkA receptor in the plasma membrane and phosphorylates intracellular TrkA tyrosine kinase, which activates downstream signaling to elongate neurites and differentiate PC12 cells into neural-like cells. Another mechanism of TRPV1 receptor-mediated differentiation is known; the TRPV1 receptor is reported to be upregulated by activation of the TrkA receptor[17]. Hence, k252a, an inhibitor of the TrakA receptor, was used to investigate the effects of the compound on TrakA.

A TrkA receptor inhibitor was used to investigate the mechanism of activity of **6** and **7**. The percentage of NOG in positive cells in the presence of k252a is shown in Fig.S3 A. Compounds **6** and **7**, and nobiletin as a positive control, displayed similar activity following treatment with k252a, suggesting that the NOG effects of **6** and **7** were not mediated by the TrkA pathway, and it might increase the NOG effect by binding to other receptors or passing the cell membrane and stimulating intracellular downstream signals.

To elucidate the mechanism of neurotrophic effects, specific inhibitors of various receptors and intracellular signaling molecules were used to calculate the inhibition rates under NGF-treated and

untreated conditions. Addition of the TRPV1 inhibitor capsazepine (5 μM) resulted in significant inhibition of NOG, with rates of 35.4% (NGF-) and 37.0% (NGF+) regardless of NGF presence. Similarly, the MEK inhibitor U0126 (10 μM) also significantly inhibited NOG and 37.0% (NGF+) inhibition rates. Further, the MEK inhibitor U0126 (10 μM) exhibited significant inhibitory activity, with 49.0% (NGF-) and 34.8% (NGF+) inhibition rates. By contrast, the inhibition rates in the group treated with the PI3K inhibitor LY294002 (20 nM) were only 24.4% (NGF-) and 11.0% (NGF+), and no statistically significant inhibition of NOG was observed.

The results obtained in this study show that capsazepine and U0126 significantly suppressed NOG, suggesting that the neurite-promoting effect of compound **7** is closely associated with the activation of the TRPV1 receptor and the subsequent MEK/ERK signaling pathway. This result is consistent with those reported previously[18], showing that piperine activates TRPV1 and contributes to NOG, suggesting that compound **7** similarly activates TRPV1 and contributes to NOG. Furthermore, a report[19] indicating that piperine-like alkamides promote axonal growth via BDNF expression suggests that this compound ultimately regulates gene transcription through CREB phosphorylation. Based on the above results, compound **7** likely activates MEK through TRPV1-mediated calcium influx or associated signal amplification, ultimately inducing the expression of genes related to neuroprotection and axonal growth via phosphorylation of the transcription factor CREB. This result is consistent with previous reports[20] revealing that piperine promotes ERK phosphorylation and that this effect is suppressed by PD98059 (an upstream inhibitor of MEK/ERK), supporting the idea that compound **7**, a piperine derivative, exerts its NOG effect primarily through the MEK/ERK pathway. Given the limited inhibitory effect of LY294002, the contribution of the PI3K/Akt pathway is considered relatively low compared with that of the MEK/ERK pathway. Based on these results, it is suggested that the primary axis of this mechanism of action depends on the TRPV1-MEK-ERK pathway. Verification of these hypotheses requires measuring the actual protein expression. These previous findings indicate that compound **7** likely induces dendritic extension in PC12 cells via a mechanism similar to that of piperine. Furthermore, because compound **7** exhibits enhanced activity compared with piperine, its affinity for the target protein and potency increase.

Animal test

Weight changes were measured in all groups during the experimental period (Fig. S25), revealing a gradual weight increase associated with aging in all the groups. Compared with the control group, no significant weight changes were observed in the scopolamine monotherapy or compound **7** administration groups. Similarly, no significant weight changes were observed in any of the groups during the corticosterone administration. The weight gain after drug administration indicates that this compound does not exhibit significant toxicity in mice.

Compound **7** exerted neurotrophic effects. However, whether they exhibit similar activities in vivo remains unclear. Therefore, we investigated potential memory-improving effects in animal experiments using mice.

In this study, we used a scopolamine-induced model that reflects acetylcholine system dysfunction to evaluate the effects of this derivative on the cholinergic system. Furthermore, using a corticosterone-induced model that is closely associated with stress-induced secondary neuronal degeneration, we examined whether the NOG effects observed in the cell culture could provide a therapeutic intervention for hippocampal dysfunction in vivo.

The Barnes maze test was used to evaluate spatial learning and memory. Figure 7B shows the progression of escape latency during the memory-formation period (Day 1–5). During the memory formation period, the control group exhibited progressively shorter escape latencies, indicating successful spatial learning. Conversely, the scopolamine-treated group displayed prolonged escape latencies throughout the study period compared with the control group. No significant improvement was observed even on day 5, confirming impaired spatial learning function. The compound **7** (10 mg/kg) group tended toward reduced escape latency during the latter half of the memory formation period (days 4– 5), ultimately shortening it to approximately 40 s. Conversely, the compound **7** (20 mg/kg)-treated group exhibited latencies comparable to or exceeding those of the scopolamine group throughout the memory formation period.

To evaluate the effect of compound **7** on spatial learning and memory abilities in the CORT(corticosterone)-induced memory impairment model mice, the Barnes maze test was also conducted. Figure 7A shows the change in escape latency during the memory-formation period (Day 1–5). During the memory formation period, the control group exhibited shortened escape latency in each trial, indicating successful spatial learning acquisition. By contrast, the CORT-treated group displayed persistently high escape latencies throughout the experimental period, with no significant shortening, even on day 5, confirming a marked inhibition of spatial learning acquisition. By contrast, the compound **7** (5 mg/kg) group exhibited a tendency toward a shorter latency than the CORT group, starting from day 2 of the memory formation period. By days 4 and 5, the latency in this group had recovered to control levels. Although a certain degree of shortening was also observed in the 10 mg/kg group, the learning progression was slower than that in the 5 mg/kg group. These results suggest that a concentration of 5 mg/kg of compound **7** is efficacious. Compound **7** improved memory impairment induced by both scopolamine and corticosterone and exhibited stronger activity against corticosterone administration than scopolamine administration. This result suggests that compound **7** suppresses stress-induced memory impairment, rather than acetylcholine-mediated memory impairment.

Conclusion

Eight compounds were isolated from *P.retrofractum* 70% EtOH extracts. Among them, seven compounds (**2**–**7**) were isolated from the hexane extract, and one compound (**1**) was isolated from the EtOAc-soluble fraction. Seven compounds (**1**,**3**–**7**), including piperine, were alkaloids, and all compounds were piperine derivatives with a methylenedioxyphenol skeleton.

Cell tests using each *P.retrofractum* extract showed that the hexane extract had a significant NOG effect. Two alkaloids (**6** and **7**) isolated from the *P.retrofractum* hexane extract displayed significant NOG effects. These results suggest that the presence of the piperidine skeleton, the number of double bonds, and the length of the carbon chain are important for NOG activity. The NOG effect of **6** and **7** was not suppressed by K252A, an inhibitor of TrakA, a receptor for NGF. This suggests that **6** and **7** stimulate NOG without the NGF receptor and might increase the NOG effect by binding to the other receptor or passing the cell membrane and stimulating the intracellular downstream signals. Subsequent testing with TRPV1 and downstream PI3K/MEK inhibitors revealed that the activity of compound **7** was significantly reduced by both the TRPV1 and MEK inhibitors. This suggests that compound **7** exerts its activity by activating the TRPV1 and MEK pathways. Further studies are needed to elucidate the mechanism of action of **6** and **7**. One of the structure-activity relationships of piperidine compounds on NOG activity in PC12 cells was clarified. Furthermore, the oral administration of compound **7** improved memory impairment induced by scopolamine and corticosterone in mice. These results provide important insights into the functionality and contributing components of *P. retrofractum*.

Materials and methods

General Procedures

Nuclear magnetic resonance (NMR) spectra were measured in chloroform-d using a JEOL ECA-600NMR (JEOL, Tokyo, Japan). Matrix-assisted laser desorption/ionization time-of-flight (MALDI-TOF-MS) spectra were measured using a Shimadzu Biotech AXIMA-Resonance spectrometer (Shimadzu Corporation, Kyoto, Japan). The isolated compounds were mixed with the matrix (2,3-dihydroxybenzoic acid in methanol, 10 mg/mL) and loaded onto a 384-well MALDI sample plate. High-performance liquid chromatography (HPLC; Shimadzu Corporation) analysis was performed on a reversed-phase column (Inertsil ODS-3 column, 4.6 mm Φ × 250 mm L; GL sciences, Tokyo, Japan) equipped with an SPD-M20A photodiode array detector (Shimadzu Corporation) to confirm the purity of the isolated compounds. Preparative HPLC, equipped with a 880-PU pump, 875-UV detector, and an Inertsil® ODS-3 column (20 mm Φ × 250 mm L; GL sciences) was conducted to obtain highly purified compounds.

Reagents

All reagents used in this study were showed as follow:

D-MEM (High-glucose, with L-glutamate and phenol red)

(Wako pure chemical industries, 044-29765, Lot No. DML7025)

HORSE SERUM (HS, gibco®, REF : 16050-122, Lot No. 1861231)

FETAL BOVINE SERUM

(FBS, biosera, Cat No. : FB-1345/500, Lot No. 015BS281)

Penicillin G (MP Biomedicals, Inc., Cat No. 194536, Lot No. QR11865)

Streptomycin (MP Biomedicals, Inc., Cat No. 194541, Lot No. R16034)

KCl (Nacarai tesque, Kyoto, Japan, Code 285 – 14, Lot No. M9E36640)

KH_2PO_4 (Wako pure chemical industries, 162-22555, Lot No. TSQ6374)

$Na_2HPO_4 \cdot 12H_2O$ (Nacarai tesque, 31723-35, Lot No. M8H5257)

NaCl (Wako pure chemical industries, 191–01665, Lot No. PTF1598)

Paraformaldehyde

(Tokyo chemical industry, Tokyo, Japan, 30525-89-4, Lot No.P33SNSA)

0.25% Trypsin-EDTA (Invitrogen GIBCO, Cat No. 25200-072, Lot No. 2192969)

Cellmatrix® Type I-C (Nitta Gelatin, Lot No. 200910)

NGF (Alomone, N-240)

Trypan blue (Wako pure chemical industries, 207–03252, Lot No. CEE3449)

Blood cell counter

(Cyber Intelligence System Inc., Gifu, Japan, 11B1X00013000015)

10 cm cell culture dish (FALCON, REF : 353003)

6 cm cell culture dish (FALCON, REF : 353004)

96 well plate (Corning Incorporated, 354407, REF : 356407)

Dimethyl sulfoxide (Wako pure chemical industries, 043-07216, Lot No. TWH0745)

Olympus CKX41 microscope (Olympus, Osaka, Japan)

Plant Material

The dried powder of *P. retrofractum* was purchased from S□B Foods Inc. (Tokyo, Japan)

Extraction of P. retrofractum dried powder

Dried *P. retrofractum* powder (approximately 2.4 kg) was extracted with 70% Ethanol (EtOH) water (v/v) on a rotary shaker (NR-20, TAITEC, Saitama, Japan) for 24 hours at room temperature. This extraction was repeated twice. The solvent was removed under reduced pressure to obtain the EtOH extract. The EtOH extract(43.6 g) was successively extracted with hexane, diethyl ether, ethyl acetate (EtOAc) and methanol (MeOH), and each solution was concentrated *in vacuo* to obtain each soluble extract.

Isolation and identification of 1–7

Compounds **1**–**7** were isolated by the method in Fig. 1. Yellow crystal (**1**; 2.2 g) was obtained from EtOAc extract. The crystal was subjected to HPLC analysis to confirm the purity and then, NMR and MALDI-TOF MS analysis was conducted to elucidate the structure of isolated compound.

The hexane extract (17 g) was subjected to normal-phase silica gel column chromatography (80 mmΦ × 430 mml;Flow rate: 2.2 ml/min)and eluted with gradient of n-hexane/EtOAc (8:2→2:8 v/v) to obtain 13 fractions (HFr.1–13). TLC analysis was conducted for the fractionation and each fraction was subjected to HPLC analysis.

Yellow crystal (**2**; 80.0 mg) was obtained from HFr. 6. The isolated compounds were identified by using NMR and MALDI-TOF MS analysis.

HFr.11 was solved in 800 µl MeOH, and then subjected to Preparative HPLC (MeOH : 0.05% TFA aq. = 85%:15%→90%:10%) to obtain highly purified compounds(**3**; 24.3 mg, **4**; 51.7 mg). The isolated compounds were identified by using NMR and MALDI-TOF MS analysis.

HFr.13 (2.0 g) was subjected to normal-phase silica gel column chromatography (50 mmΦ × 350 mml) and eluted with gradient of n-hexane/EtOAc (7:3→3:7 v/v) to obtain eleven fractions (HFr.13 − 1-11). TLC analysis was conducted for the fractionation and each fraction was analyzed by HPLC.

HFr.13 − 10(100 mg) was solved in 1000 µl MeOH, and then subjected to Preparative HPLC (MeOH : 0.05% TFA aq. = 60%:40%→100%:0%) to obtain highly purified compound (**5**; 30.1 mg). The obtained compound was identified by using NMR and MALDI-TOF MS analysis.

HFr.13 − 8 (100 mg) was solved in 1000 µl MeOH, and then subjected to Preparative HPLC (MeOH : 0.05% TFA aq. = 80%:20%→80%:20%) to obtain highly purified compounds (**6**; 9.1 mg, **7**; 71.9 mg). The obtained compounds were identified by using NMR and MALDI-TOF MS analysis.

Elucidation of the structures of compounds from P. retrofractum

Compound **1** was obtained as yellow crystal and determined as the molecular formula $C_{17}H_{19}NO_3$ by MALDI-TOF-MS (positive ion mode) m/z: 308.1263$[M + Na]^+$, implying alkaloid containing one nitrogen. Compound **1** was identified as piperine comparing with the previous NMR data[21].The COSY and HMBC correlations supported the structure (Fig. 2).

1

Yellow crystal; MALDI-TOF-MS m/z 308.1263 $[M + Na]^+$(calcd for $C_{17}H_{19}NO_3Na$, 308.1263); ^{1}H-NMR (CHLOROFORM-D, JEOL EC, 600 MHz)δ_H (ppm) 1.56 (4H, m, C2"-H, C4"-H), 1.63 (2H, m, C3"-H), 3.49 (2H, br s, C1"-H), 3.60 (2H, br s, C5"-H), 5.93 (2H, s, OCH_2O), 6.41 (1H, d, J = 14.43 Hz, C2-H), 6.70 (1H, m, C4-H), 6.71 (1H, m, C5-H), 6.74 (1H, d, J = 8.25 Hz, C5´-H), 6.86 (1H, dd, J = 1.37, 7.56 Hz), 6.94(1H, s, C2´-H), 7.36(1H, m, C3-H); ^{13}C-NMR (CHLOROFORM-D, JEOL EC, 150 MHz)δ_C (ppm) 24.7 (C-4"), 25.7 (C-3"), 26.8 (C-2"), 43.3 (C-1"), 46.9 (C-5"), 101.3 (OCH_2O), 105.7 (C-2´), 108.5 (C-5´), 120.1 (C-2), 122.5 (C-6´), 125.4 (C-4), 131.0 (C-1´), 138.2 (C-5), 142.5 (C-3), 148.1 (C-3´), 148.2 (C-4´), 165.4 (C-1)

Compound **2** was obtained as yellow crystal and determined as the molecular formula $C_{13}H_{12}O_4$ by MALDI-TOF-MS (positive ion mode) m/z: 232.0579$[M + Na]^+$.

Compound **2** was identified as methyl piperate via comparing with the previous NMR data[22]. The COSY and HMBC correlations supported the structure (Fig. 2).

2

Yellow crystal; MALDI-TOF-MS m/z 255.0579 $[M + Na]^+$(calcd for $C_{13}H_{12}O_4Na$, 255.0628); ^{1}H-NMR (CHLOROFORM-D, JEOL EC, 600 MHz)δ_H (ppm) 3.75 (3H, s, C1"-H), 5.93 (1H, d, J = 15.12 Hz, C-2), 5.96 (2H, s, OCH_2O), 6.67 (1H, dd, J = 11.00,15.81 Hz, C4-H), 6.76 (1H, d, J = 7.56 Hz, C6´-H), 6.78 (1H, d, J = 15.81, C5-H), 6.89 (1H, dd, J = 1.37, 7.56 Hz, C5´-H), 6.97 (1H, d, J = 1.72 Hz, C2´-H), 7.40 (1H, dd, J = 11.00, 15.12 Hz, C3-H); ^{13}C-NMR (CHLOROFORM-D, JEOL EC, 150 MHz)δ_C (ppm), 51.6 (C-1"), 101.5 (OCH_2O), 106.0 (C-2´), 108.6 (C-5´), 120.0 (C-2), 123.0 (C-6´), 124.6 (C-4), 130.6 (C-1´), 140.4 (C-5), 145.1 (C-3), 148.4 (C-3´), 148.7 (C-4´), 167.7 (C-1)

Compound **3** was obtained as colorless crystal and determined to have molecular formula $C_{22}H_{29}NO_3$ by MALDI-TOF-MS (positive ion mode) m/z: 378.2048$[M + Na]^+$, implying alkaloid containing one nitrogen. Compound **3** was identified as pipercide via comparing with the previous NMR data[23]. The COSY and HMBC correlations supported the structure (Fig. 2).

3

Colorless crystal; MALDI-TOF-MS m/z 378.2048 $[M + Na]^+$(calcd for $C_{22}H_{29}NO_3Na$, 378.2040); ^{1}H-NMR (CHLOROFORM-D, JEOL EC, 600 MHz)δ_H (ppm) 0.92 (3H, d, J = 6.87 Hz, C3"-H), 0.92 (3H, d, J = 6.87 Hz, C4"-H), 1.46 (2H, m, C7-H), 1.46 (2H, m, C8-H), 1.79 (1H, m, C2"-H), 2.17 (2H, m, C6-H), 2.17 (2H, m, C9-H), 3.16 (2H, t, J = 6.87 Hz, C1"-H), 5.74 (1H, d, J = 15.12 Hz, C-2), 5.93 (2H, s, OCH_2O), 6.04 (1H, m, C5-H), 6.04 (1H, m, C10-H), 6.13(1H, dd, J = 11.00,15.12 Hz, C4-H), 6.28(1H, d, J = 15.81 Hz, C-11), 6.72 (1H, d, J = 7.56 Hz, C-5´), 6.75 (1H, dd, J = 2.06, 7.56 Hz, C6´-H), 6.89 (1H, d, J = 1.37 Hz, C2´-H), 7.19 (1H, dd, J = 10.31, 15.12 Hz, C3-H); ^{13}C-NMR (CHLOROFORM-D, JEOL EC, 150 MHz)δ_C (ppm), 20.4 (C-3"), 20.4 (C-4"),

28.6 (C-7), 29.0 (C-2"), 29.3(C-8), 33.0 (C-9), 33.1 (C-6), 47.3 (C-1"), 101.2 (OCH_2O), 105.7 (C-2´), 108.5 (C-5´), 120.6 (C-6´), 122.2 (C-2), 128.7 (C-4), 129.3 (C-10), 129.9 (C-11), 132.7 (C-1´), 141.5 (C-3´), 143.1 (C-5), 146.9 (C-4´), 148.3(C-3´), 167.7 (C-1)

Compound **4** was obtained as colorless crystal and determined to have molecular formula $C_{24}H_{32}NO_3$ by MALDI-TOF-MS (positive ion mode) m/z: 406.2352 $[M + Na]^+$, implying alkaloid containing one nitrogen. Compound **4** was identified as guineesine via comparing with the previous NMR data[23]. The COSY and HMBC correlations supported the structure (Fig. 2).

4

Colorless crystal; MALDI-TOF-MS m/z 406.2352 $[M + Na]^+$ (calcd for $C_{24}H_{32}NO_3Na$, 406.2353); ^{1}H-NMR (CHLOROFORM-D, JEOL EC, 600 MHz)δ_H (ppm) 0.90 (3H, d, J = 6.87 Hz, C3"-H), 0.91 (3H, d, J = 6.87 Hz, C4"-H), 1.30 (2H, m, C8-H), 1.30 (2H, m, C9-H), 1.41 (2H, m, C7-H), 1.41 (2H, m, C10-H), 1.79 (1H, m, C2"-H), 2.14 (2H, m, C6-H), 2.14 (2H, m, C11-H), 3.14 (2H, t, J = 6.87 Hz, C1"-H), 5.78 (1H, d, J = 15.12 Hz, C-2), 5.91 (2H, s, OCH_2O), 6.03 (1H, m, C5-H), 6.03 (1H, m, C12-H), 6.11 (1H, dd, J = 11.00,15.12 Hz, C4-H), 6.26(1H, d, J = 15.81 Hz, C13-H), 6.71 (1H, d, J = 7.56 Hz, C5´-H), 6.74 (1H, dd, J = 2.06, 8.25 Hz, C6´-H), 6.88 (1H, d, J = 2.06 Hz, C2´-H), 7.17 (1H, dd, J = 10.31, 15.12 Hz, C3-H); ^{13}C-NMR (CHLOROFORM-D, JEOL EC, 150 MHz)δ_C (ppm), 20.4 (C-3"), 20.4 (C-4"), 28.9 (C-2"), 29.0 (C-8), 29.2(C-9), 29.3(C-7), 29.6(C-10), 33.1 (C-11), 33.2 (C-6), 47.2 (C-1"), 101.2 (OCH_2O), 105.6 (C-2´), 108.5 (C-5´), 120.5 (C-6´), 122.2 (C-2), 128.6 (C-4), 129.6 (C-5), 129.6(C-13), 132.7 (C-1´), 141.4 (C-3´), 143.2 (C-12), 146.8 (C-4´), 148.2(C-3´), 166.8 (C-1)

Compound **5** was obtained as yellow oil and determined to have molecular formula $C_{17}H_{21}NO_3$ by MALDI-TOF-MS (positive ion mode) m/z: 288.1549 $[M + H]^+$, implying alkaloid containing one nitrogen. Compound **5** was identified as piperanine via comparing with the previous NMR data[21]. The COSY and HMBC correlations supported the structure (Fig. 2).

5

Yellow oil,; MALDI-TOF-MS m/z 288.1549 $[M + H]^+$ (calcd for $C_{17}H_{22}NO_3$, 288.1594); ^{1}H-NMR (CHLOROFORM-D, JEOL EC, 600 MHz)δ_H (ppm) 1.54 (4H, m, C2"-H, C4"-H), 1.63 (2H, m, C3"-H), 2.46 (2H, m, C4-H), 2.69 (2H, m, C5-H), 3.40 (2H, br s, C5"-H), 3.58 (2H, br s, C1"-H), 5.90 (2H, s, OCH_2O), 6.20 (1H, d, J = 15.12 Hz, C2-H), 6.61 (1H, dd, J = 1.37, 7.56 Hz, C6´-H), 6.66 (1H, d, J = 1.41, Hz), 6.71(1H, s, C5´-H), 6.79(1H, m, C3-H); ^{13}C-NMR (CHLOROFORM-D, JEOL EC, 150 MHz)δ_C (ppm) 24.7 (C-3"), 25.6 (C-2"), 25.6 (C-4"), 34.6 (C-5), 34.7(C-4), 43.3 (C-1"), 47.1 (C-5"), 100.9 (OCH_2O), 108.3 (C-5´), 109.0(C-2´), 121.3 (C-6´), 121.4 (C-2), 135.1 (C-1´), 144.4 (C-3), 145.4 (C-4´), 147.7 (C-3´), 165.8 (C-1)

Compound **6** was obtained as yellow oil and determined to have molecular formula $C_{21}H_{25}NO_3$ by MALDI-TOF-MS (positive ion mode) m/z: 340.1931$[M + H]^+$, implying alkaloid containing one nitrogen.

Compound **6** was identified as dehydropipernonaline via comparing with the previous NMR data[24]. The COSY and HMBC correlations supported the structure (Fig. 2).

6

Yellow oil; MALDI-TOF-MS m/z 340.1931 $[M + H]^+$ (calcd for $C_{21}H_{26}NO_3$, 340.1907); ^{1}H-NMR (CHLOROFORM-D, JEOL EC, 600 MHz)δ_H (ppm) 1.54–1.65 (2H, m, C3"-H), 1.54–1.65 (2H, m, C4"-H), 1.54–1.65 (2H, m, C5"-H), 2.30 (2H, m, C6-H), 2.30 (2H, m, C7-H), 3.47(2H, br s, C5"-H), 3.60(2H, br s, C1"-H), 5.91 (2H, s, OCH_2O), 6.01 (1H, m, C-8), 6.06 (1H, m, C5-H), 6.20 (1H, dd, J = 11.0,15.12 Hz C4-H), 6.25 (1H, d, J = 15.12 Hz, C-2), 6.30 (1H, d, J = 15.81 Hz, C-9), 6.72 (1H, d, J = 8.25 Hz, C2´-H), 6.73 (1H, dd, J = 2.06, 7.56 Hz, C6´-H), 6.87 (1H, d, J = 1.37 Hz, C2´-H), 7.23 (1H, dd, J = 11.0, 15.12 Hz, C3-H); ^{13}C-NMR (CHLOROFORM-D, JEOL EC, 150 MHz)δ_C (ppm), 24.8 (C-3"), 25.8 (C-4"), 26.8 (C-2"), 32.3 (C-6), 33.0 (C-7), 43.4(C-1"), 47.0(C-5"), 101.1 (OCH_2O), 105.6 (C-2´), 108.4 (C-5´), 119.1 (C-2), 120.5 (C-6´), 127.9 (C-8), 129.5 (C-4), 130.3 (C-9), 132.3 (C-1´), 141.3 (C-5), 142.7 (C-3), 146.9(C-4´), 148.1 (C-3´), 165.8 (C-1)

Compound **7** was obtained as yellow oil and determined to have molecular formula $C_{21}H_{27}NO_3$ by MALDI-TOF-MS (positive ion mode) m/z: 342.2037$[M + H]^+$, implying alkaloid containing one nitrogen. Compound **7** was identified as pipernonaline via comparing with the previous NMR data[21]. The COSY and HMBC correlations supported the structure (Fig. 2).

7

Yellow oil; MALDI-TOF-MS m/z 342.2037 $[M + H]^+$ (calcd for $C_{21}H_{28}NO_3$, 342.2064); ^{1}H-NMR (CHLOROFORM-D, JEOL EC, 600 MHz)δ_H (ppm) 1.48 (2H, m, C5-H), 1.48 (2H, m, C6-H), 1.55 (2H, m, C2"-H), 1.55 (2H, m, C4"-H), 1.63 (2H, m, C3"-H), 2.20 (2H, m, C4-H), 2.17 (2H, m, C7-H), 3.46(2H, br s, C5"-H), 3.58(2H, br s, C1"-H), 5.90 (2H, s, OCH_2O), 6.01 (1H, m, C-8), 6.23 (1H, d, J = 15.12 Hz, C2-H), 6.26 (1H, d, J = 15.8 Hz, C-9), 6.73 (1H, d, J = 7.56 Hz, C5´-H), 6.74 (1H, dd, J = 1.37, 7.56 Hz C6´-H), 6.81(1H, m, C3-H), 6.87 (1H, d, J = 1.37 Hz, C2´-H),; ^{13}C-NMR (CHLOROFORM-D, JEOL EC, 150 MHz)δ_C (ppm), 24.7 (C-3"), 25.6 (C-4"), 26.7 (C-2"), 28.0 (C-6), 29.0 (C-5), 32.5 (C-4),32.7 (C-7), 43.3(C-1"), 47.0(C-5"), 101.0 (OCH_2O), 105.4 (C-2´), 108.3 (C-5´), 120.3 (C-6´), 120.4 (C-2), 128.9 (C-8), 129.7 (C-9), 132.4 (C-1´), 146.0 (C-3), 146.6 (C-4´), 148.0 (C-3´), 165.9 (C-1)

Collagen Coating of cell culture Dishes

Collagen (Cellmatrix Type I-C) was diluted 10-fold with HCl water at pH 3. The solution was poured into cell culture dishes and leaved to stand for 60 minutes at room temperature. After standing, the solution was aspirated, and the dishes were aseptically dried at room temperature. After washing twice with cell culture medium or PBS(-), the dishes were used.

Culture of PC12 cells

PC12 cells were cultured in DMEM medium containing 10% HS, 5% FBS, 100U/ml penicillin G and 100µg/ml streptomycin. The cells were incubated at 37°C in humidified atmosphere of 5% CO_2 on 10 cm collagen coated dish. The culture medium was changed once every two or three days.

Neurite outgrowth (NOG) activity

NOG activity evaluation was performed in 96 well plate at a density of 5.0 x 10^4 cells/well. After 24h incubation, the media is replaced by the sample solutions in fresh medium with or without 5 ng/ml NGF. The cells were incubated for 72h at 37°C in humidified atmosphere of 5% CO_2. Nobiletin (50,100 µM) was used as a positive control. In order to determine the number of NOG positive cells, cells were fixed by 4% paraformaldehyde solution for 10 min. at room temperature. NOG was observed using Olympus CKX41 microscope. Cells with neurites that were more than twice as long as the cell body were defined positive cells. NOG activity was calculated as a ratio of the number of positive cells to total cell count.

$2\ell_1<\ell_2$: Neurite outgrowth positive cells

ℓ_2: The length of cell including dendrite

ℓ_1: The length of cell without dendrite

Inhibitory test

Inhibitory test was performed in 96 well plate at a density of 5.0 x 10^4 cells/well. After 22h incubation, the media is replaced by fresh medium including inhibitors (400 µM k252a, 5 µM capsazepine, 10 µM U0126, and 20 µM LY294002). After 2 hours incubation, the media is replaced by the sample solutions in fresh medium with 5 ng/ml NGF. The cells were incubated for 72h at 37°C in humidified atmosphere of 5% CO_2. In order to determine the number of NOG positive cells, cells were fixed by 4% paraformaldehyde solution for 10 min. at room temperature. NOG was observed using Olympus CKX41 microscope.

Animal test

All animal experiments were approved by the Ethics Committee of Gifu University and conducted in accordance with the guidelines (Approval No.: AG-P-N-20250148, 2022 – 111). Five-week-old ICR mice were obtained from SLC Japan Co., Ltd. Mice were housed with free access to food (Oriental Yeast Co., Ltd., MF Solid) and water under a 12-hour light cycle at room temperature (24°C ± 1°C) and relative humidity (60 ± 10%).

Two clinically relevant disease models using scopolamine and corticosterone were adopted to evaluate the pharmacological effects of the piperine derivative. All behavioral tests were evaluated by individuals unfamiliar with all groups.

Effects of Compound 7 on Scopolamine-Induced Memory Impairment in Mice

Twenty-four mice (strain: ICR, 5 weeks old) were used. They were divided into the Control group, the scopolamine group, the compound **7** (10 mg/kg) group, and the compound **7** (20 mg/kg) group. The control group received the control solution (saline + 0.1% DMSO, 0.1% Tween-80). The scopramine group and compound **7** groups received a 4 mg/kg scoporamine solution (saline + 0.1% DMSO, 0.1% Tween-80) subcutaneously once daily for 10 days. The administration method involved subcutaneous injections 30 minutes after oral administration, followed by the Barnes maze 30 minutes later. Compound **7** was administered orally daily. On day 9, subcutaneous administration of scopolamine was also initiated daily in addition to compound **7**. From day 9 onward, both compound **7** and scopolamine were administered, and the Barnes maze test was performed.

Effects of Compound 7 on Corticosterone-Induced Memory Impairment in Mice

Twenty-four mice (strain: ICR, 5 weeks old) were used. They were divided into Control, CORT (corticosterone-induced group), compound **7** (5 mg/kg), and compound **7** (10 mg/kg) groups. The control group received the control solution (saline + 0.1% DMSO, 0.1% Tween-80). The CORT group and compound **7** administration groups received a 50 mg/kg corticosterone solution (saline + 0.1% DMSO, 0.1% Tween-80) subcutaneously once daily. The administration method involved subcutaneous injections 30 minutes after oral administration, followed by the Barnes maze 30 minutes later. Corticosterone was administered subcutaneously daily for 46 days. Oral administration of compound 7 was initiated on day 15 of corticosterone administration and continued daily in addition to the corticosterone injections. The Barnes maze test was performed 41 days after corticosterone administration began.

Barnes Maze

The Barnes maze test was performed based on a previous report[25], [26]. The Barnes maze consists of a 92 cm diameter circular plate with 20 evenly spaced circular holes, each 5 cm in diameter. Only one hole has a dark (escape) box attached beneath the plate. Mice that dislike bright open spaces enter the escape box once they find one while peering into the holes. Spatial learning can be assessed by counting the time taken to reach the escape box and the number of times the mouse peers into holes other than the escape box (error count).

After acclimating the mice to darkness for at least 15 min, they were placed in a tube and positioned at the center of the Barnes maze for 30 s. After 30 s, the tube was removed, and the mice were allowed to explore the Barnes maze. If the mouse entered the escape box on its own, it was placed inside for 30 s starting from that point. If the mouse did not enter the escape box within 2 min, it was guided into it and placed inside for 30 s. On days 1–5, two 2.5-min trials were conducted daily. The total escape latency (time from start to entry into the escape box) was measured on days 1–5.

Statistical assay

Cell experiments were performed in triplicate (n = 3), and animal experiments were performed using six mice for each group (n = 6). Significance was analyzed using Dunnett's method by EZR. ***P < 0.001, **P < 0.01 and *P < 0.05

Declarations

Declaration of Competing Interest

The authors declare that they have no known competing financial interests in this paper.

Author Contribution

R.F. wrote the main manuscript text and conducted the experiment. Y. I. conducted the experiment. T.M. supervised the study and edited the manuscript. K.Y. supervised the study, wrote, and edited the manuscript. All authors reviewed the manuscript.

Data availability

Data will be made available on request.

References

1. Livingston G, Huntley J, Sommerlad A, et al. Dementia prevention, intervention, and care: 2020 report of the Lancet Commission. Lancet. 2020;396(10248):413–46. 10.1016/S0140-6736(20)30367-6.
2. Heese K, Jin WL, Inoue N. Nerve growth factor, neural stem cells and Alzheimer's disease. Neurosignals. 2006;15(1):1–12. 10.1159/000094383.
3. Faizul Azam. Neuroprotective Effects of Phytochemicals in Neulogical Disorders Chap. 7 Ginger Components as Anti-Alzheimer Drugs Focus on Drug Design. 2016.
4. Kaur K, Sharma R, Singh S. Bioactive composition and promising health benefits of natural food flavors and colorants: potential beyond their basic functions. Pigment Resin Technol. 2020;49(2):110–8. 10.1108/PRT-02-2019-0009.
5. Lu J, Zhou W, Dou F, Wang C, Yu Z. TRPV1 sustains microglial metabolic reprogramming in Alzheimer's disease. EMBO Rep. 2021;22(6):1–17. 10.15252/embr.202052013.
6. Dong Y, Yin Y, Vu S, et al. A distinct structural mechanism underlies TRPV1 activation by piperine. Biochem Biophys Res Commun. 2019;516(2):365–72. 10.1016/j.bbrc.2019.06.039.
7. Cui Y, Perez S, Venance L. Endocannabinoid-LTP mediated by CB1 and TRPV1 receptors encodes for limited occurrences of coincident activity in neocortex. Front Cell Neurosci. 2018;12(July):1–14. 10.3389/fncel.2018.00182.

8. Frey E, Karney-Grobe S, Krolak T, Milbrandt J, DiAntonio A. TRPV1 agonist, capsaicin, induces axon outgrowth after injury via Ca2+/PKA signaling. eNeuro. 2018;5(3):1–15. 10.1523/ENEURO.0095-18.2018.
9. Freedman P. Health, wellness and the allure of spices in the Middle Ages. J Ethnopharmacol. 2015;167:47–53. 10.1016/j.jep.2014.10.065.
10. Scapagnini G, Caruso C, Calabrese V. Therapeutic potential of dietary polyphenols against brain ageing and neurodegenerative disorders. Adv Exp Med Biol. 2010;698:27–35. 10.1007/978-1-4419-7347-4_3.
11. Guo Z, Xu J, Xia J, Wu Z, Lei J, Yu J. Anti-inflammatory and antitumour activity of various extracts and compounds from the fruits of Piper longum L. J Pharm Pharmacol. 2019;71(7):1162–71. 10.1111/jphp.13099.
12. Jiang ZY, Liu WF, Zhang XM, Luo J, Ma YB, Chen JJ. Anti-HBV active constituents from Piper longum. Bioorg Med Chem Lett. 2013;23(7):2123–7. 10.1016/j.bmcl.2013.01.118.
13. Ohno O, Watabe T, Nakamura K, et al. Inhibitory effects of bakuchiol, bavachin, and isobavachalcone isolated from piper longum on melanin production in b16 mouse melanoma cells. Biosci Biotechnol Biochem. 2010;74(7):1504–6. 10.1271/bbb.100221.
14. Desai SJ, Prabhu BR, Mulchandani NB, Aristolactams. 4,5-dioxoaporphines from Piper longum. Phytochemistry. 1988;27(5):1511–5. 10.1016/0031-9422(88)80226-7.
15. Hritcu L, Noumedem JA, Cioanca O, Hancianu M, Postu P, Mihasan M. Anxiolytic and antidepressant profile of the methanolic extract of Piper nigrum fruits in beta-amyloid (1–42) rat model of Alzheimer's disease. Published online. 2011. 10.1186/s12993-015-0059-7.
16. Greene LA, Tischler AS. Establishment of a noradrenergic clonal line of rat adrenal pheochromocytoma cells which respond to nerve growth factor. Proc Natl Acad Sci U S A. 1976;73(7):2424–8. 10.1073/pnas.73.7.2424.
17. Rodrigues TB, Ballesteros P. Journal of Neuroscience Research 85:3244–3253 (2007). J Neurosci Res. 2007;3253(April):3244–3253. 10.1002/jnr
18. Okumura Y, Narukawa M, Iwasaki Y, et al. Activation of TRPV1 and TRPA1 by black pepper components. Biosci Biotechnol Biochem. 2010;74(5):1068–72. 10.1271/bbb.90964.
19. Yun YS, Noda S, Takahashi S, Takahashi Y, Inoue H. Piperine-like alkamides from Piper nigrum induce BDNF promoter and promote neurite outgrowth in Neuro-2a cells. J Nat Med. 2018;72(1):238–45. 10.1007/s11418-017-1140-3.
20. Lee JH, Lee J, Dej-Adisai S, Hwang JS. Piperine Regulates Melanogenesis through ERK Activation and Proteasomal Degradation of MITF. Biomol Ther (Seoul). 2025;33(2):408–14. 10.4062/biomolther.2024.065.
21. Wu S, Sun C, Pei S, Lu Y, Pan Y. Preparative isolation and purification of amides from the fruits of Piper longum L. by upright counter-current chromatography and reversed-phase liquid chromatography. J Chromatogr A. 2004;1040(2):193–204. 10.1016/j.chroma.2004.03.056.

22. Venkatasamy R, Faas L, Young AR, Raman A, Hider RC. Effects of piperine analogues on stimulation of melanocyte proliferation and melanocyte differentiation. Bioorg Med Chem. 2004;12(8):1905–20. 10.1016/j.bmc.2004.01.036.
23. Khatami Z, Sarkheil P, Adhami H. Isolation and characterization of acetylcholinesterase inhibitors from Piper longum Linn. Planta Med. 2016;81(01):S1–381. 10.1055/s-0036-1596876.
24. Seung WL, Rho MC, Hye RP, et al. Inhibition of diacylglycerol acyltransferase by alkamides isolated from the fruits of Piper longum and Piper nigrum. J Agric Food Chem. 2006;54(26):9759–63. 10.1021/jf061402e.
25. Brunden KR, Zhang B, Carroll J, et al. Epothilone D improves microtubule density, axonal integrity, and cognition in a transgenic mouse model of tauopathy. J Neurosci. 2010;30(41):13861–6. 10.1523/JNEUROSCI.3059-10.2010.
26. Gawel K, Gibula E, Marszalek-Grabska M, Filarowska J, Kotlinska JH. Assessment of spatial learning and memory in the Barnes maze task in rodents-methodological consideration. Naunyn Schmiedebergs Arch Pharmacol. 2019;392(1). 10.1007/s00210-018-1589-y.

Figures

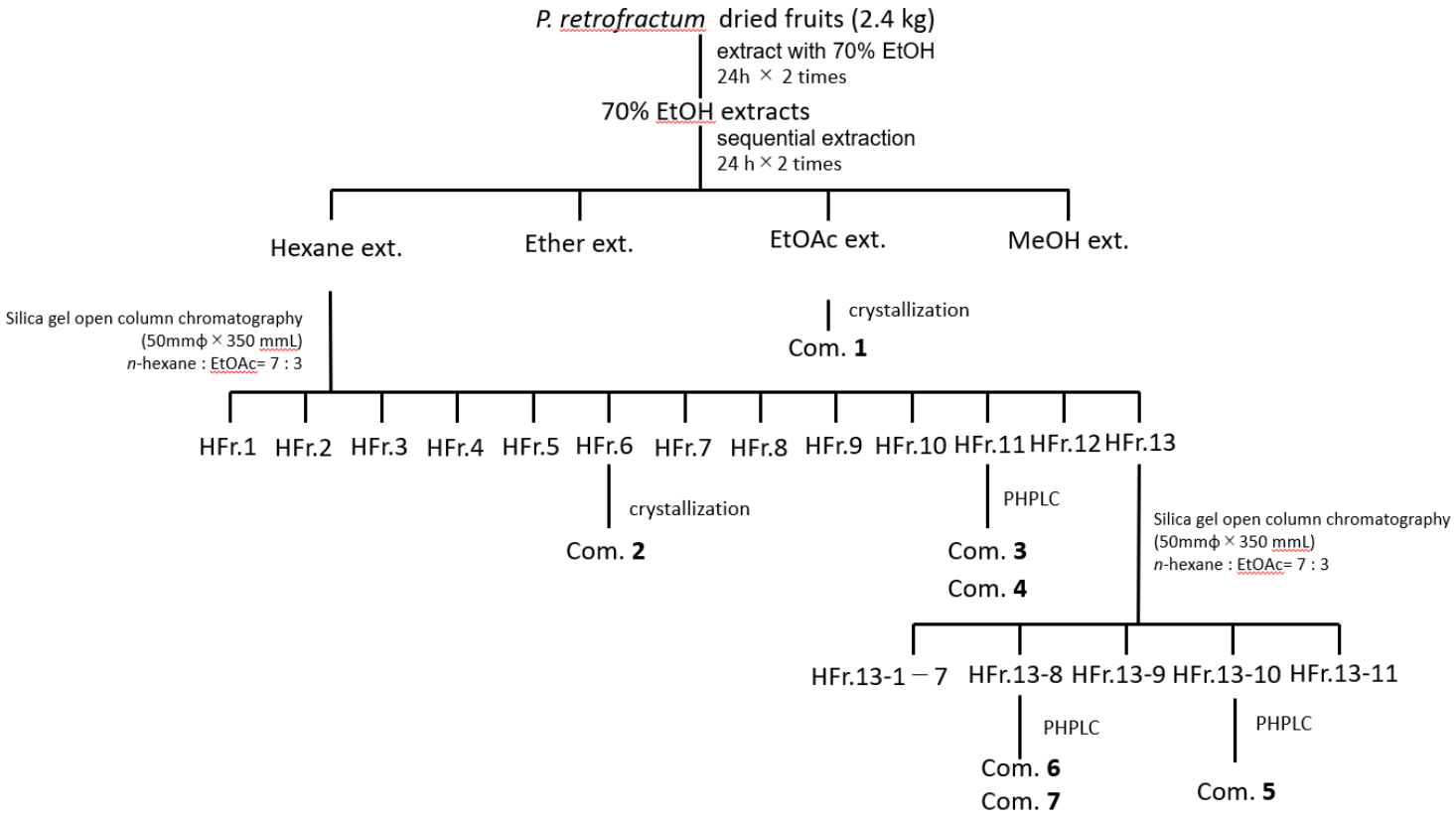

Figure 1

Isolation scheme of components from *P. retrofractum*

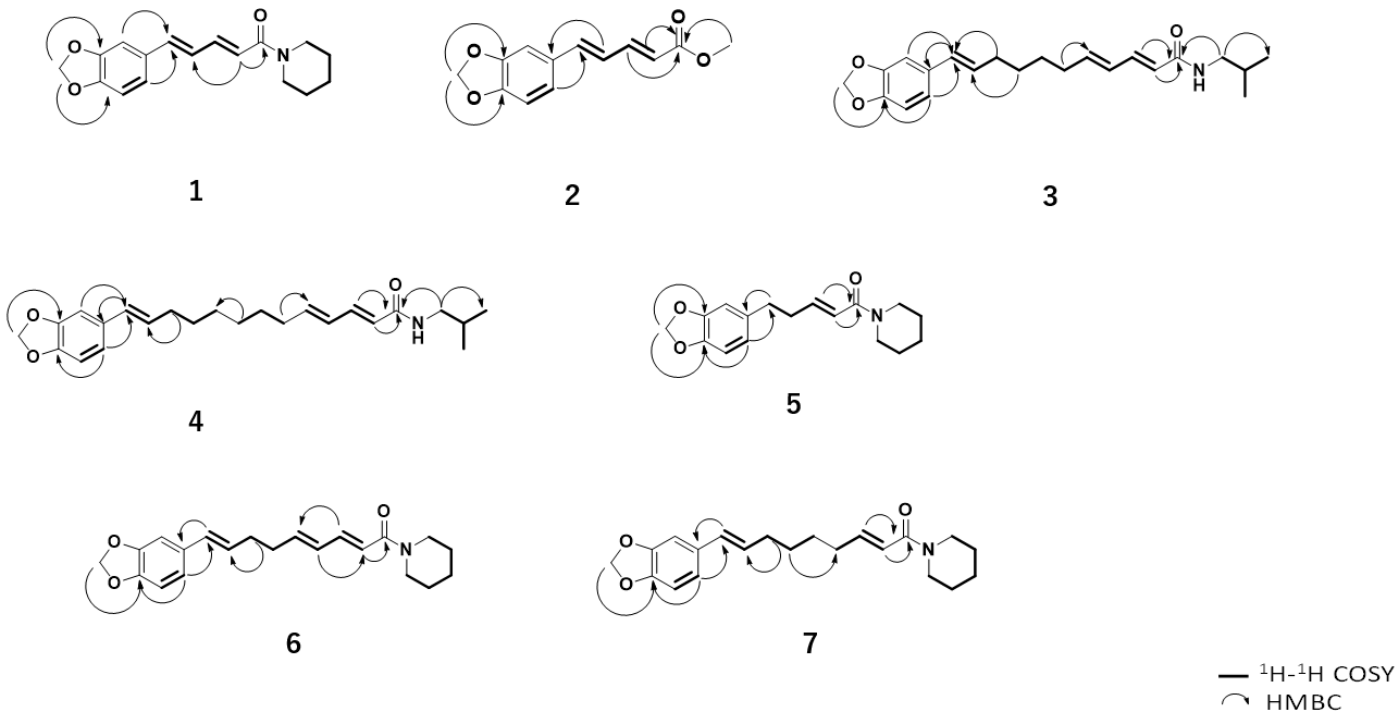

Figure 2

COSY and HMBC NMR correlations of **1**-**7**from *P. retrofractum*

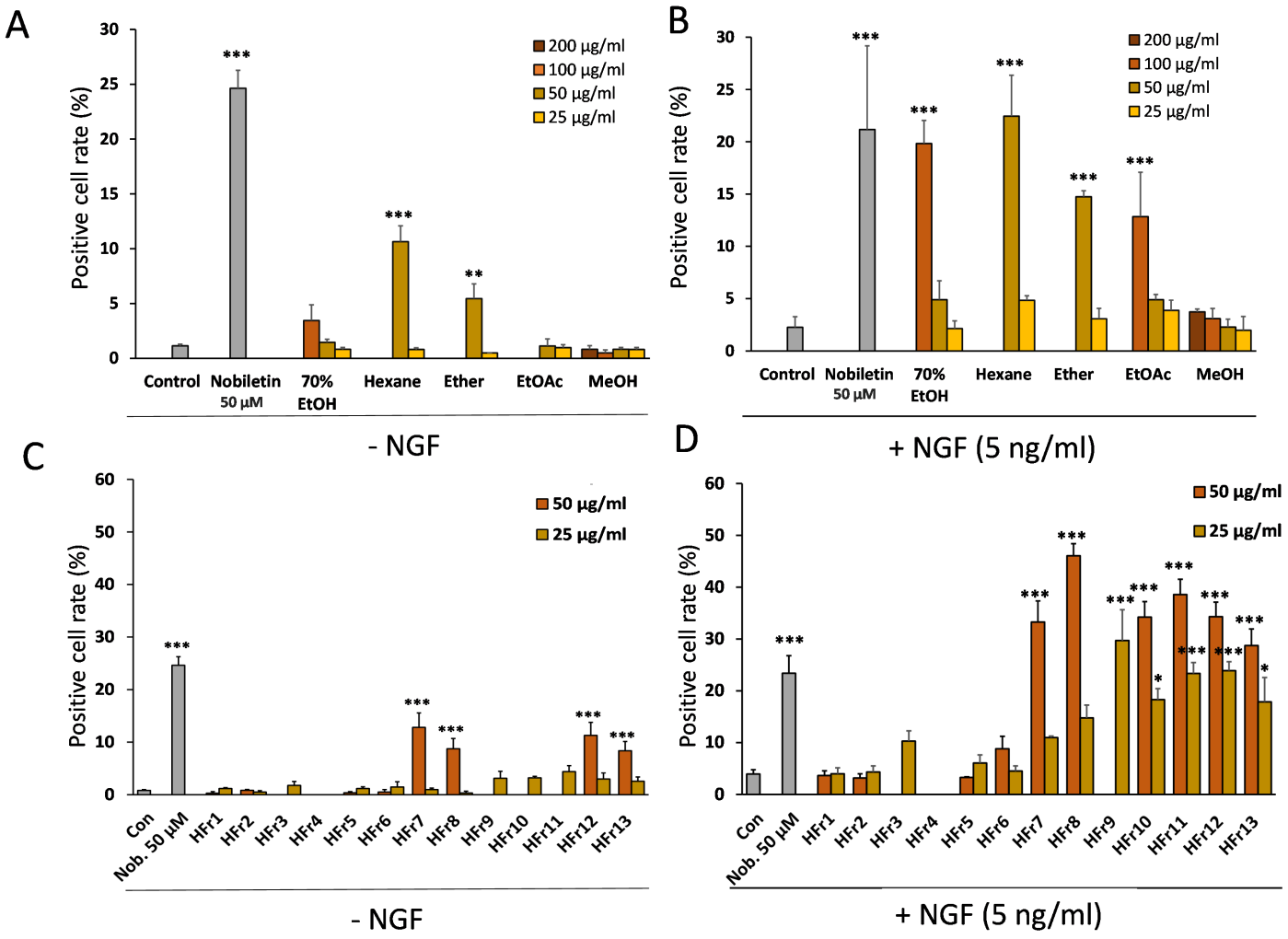

Figure 3

Rate of neurite outgrowth positive cells in PC12 cells treated with fractions from 70 % EtOH extract of *P. retrofractum*.

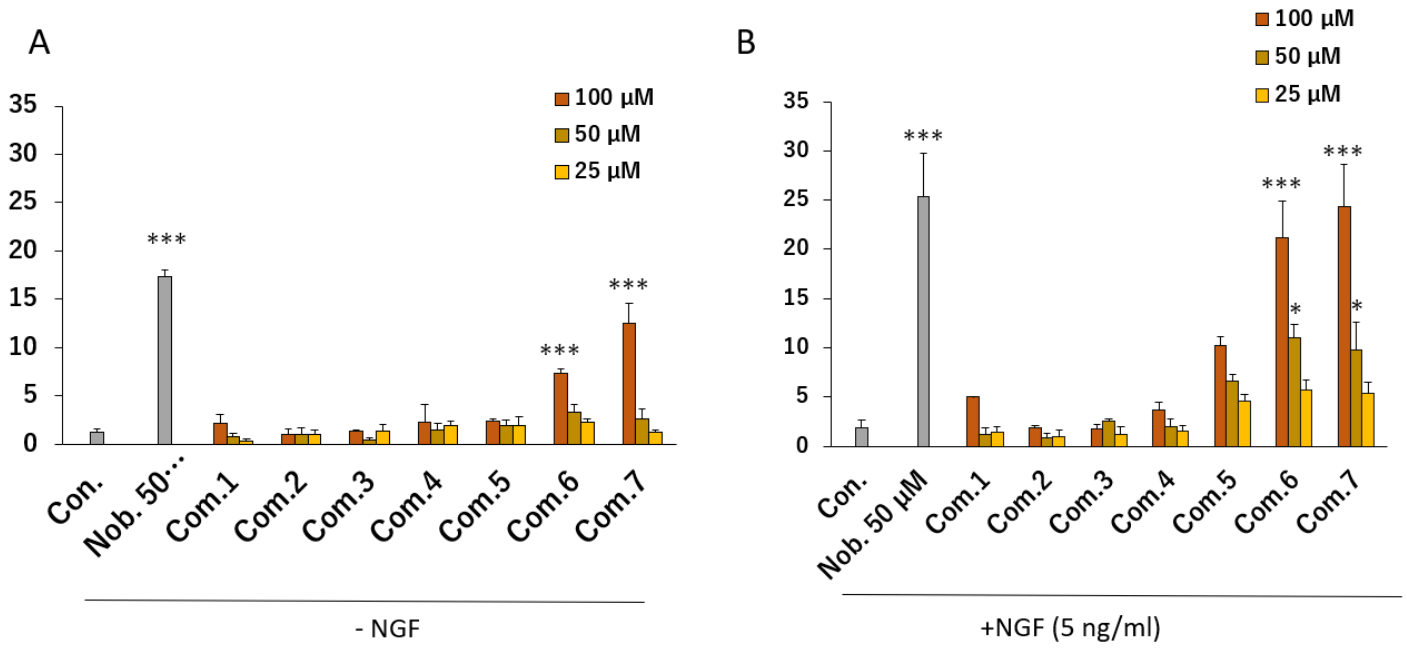

Figure 4

Rate of neurite outgrowth positive cells in PC12 cells treated with compounds from 70 % EtOH extract of *P. retrofractum*.

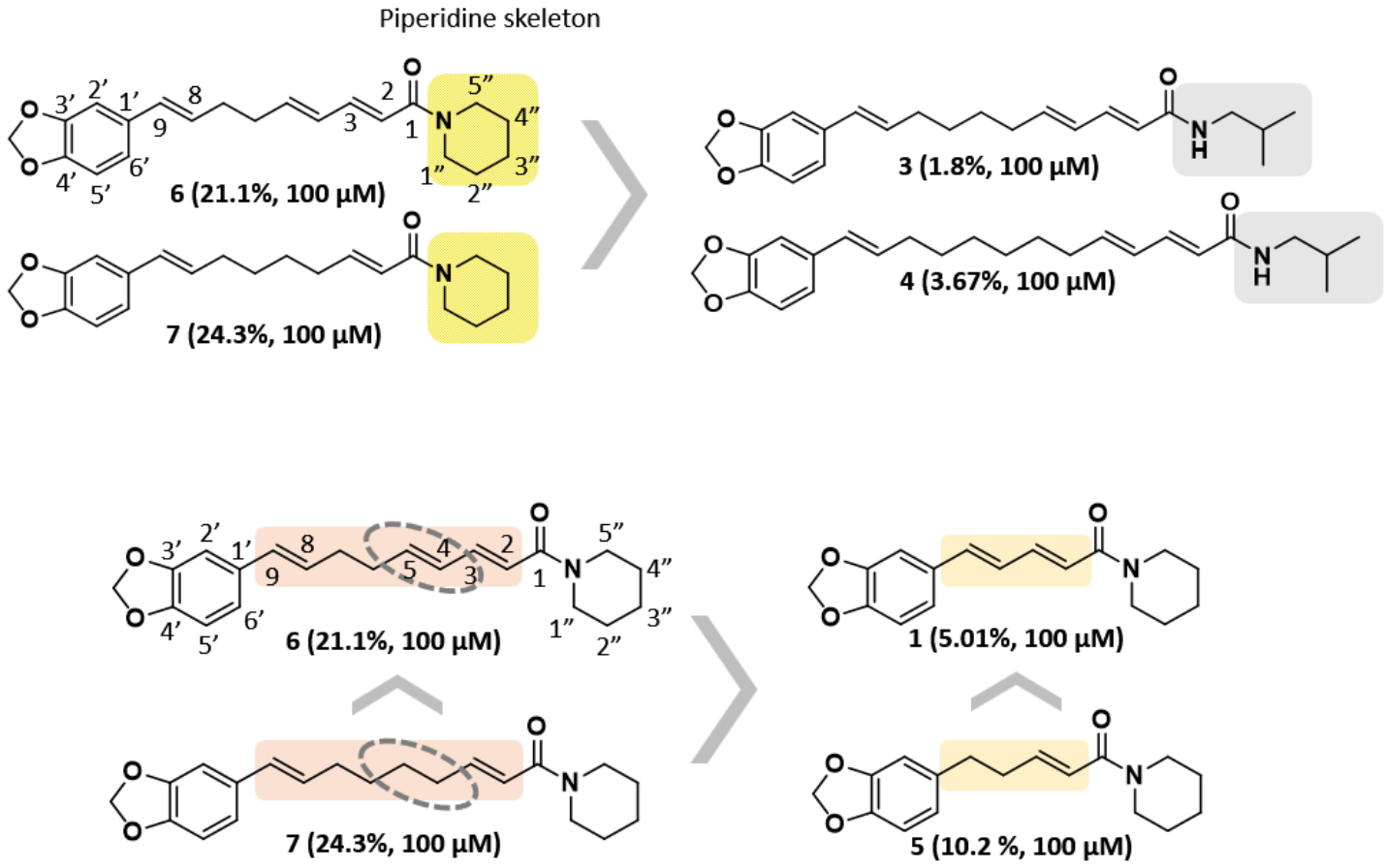

Figure 5

Structure-activity relationship of the piperine derivatives which have methylenedioxyphenol skeleton for neurite outgrowth activity.

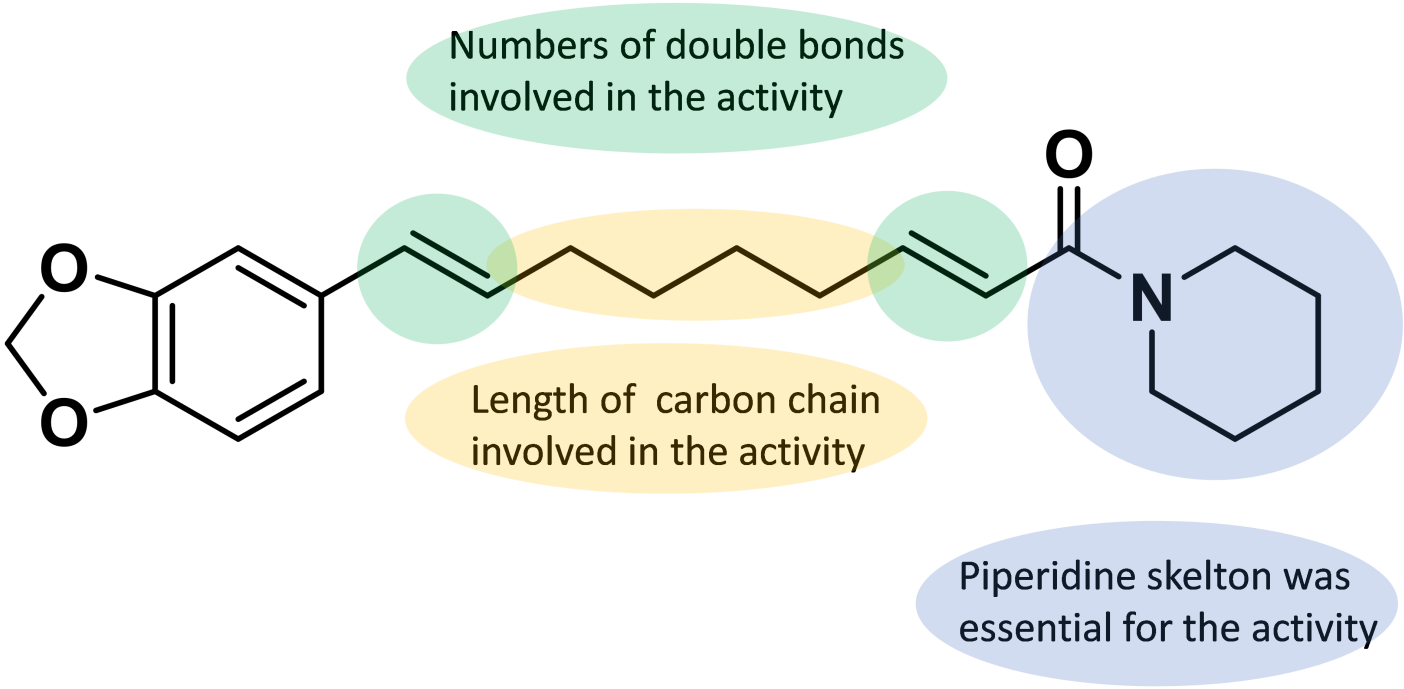

Figure 6

Summary of structure-activity relationship of the pipernonaline from *P. retrofractum*.

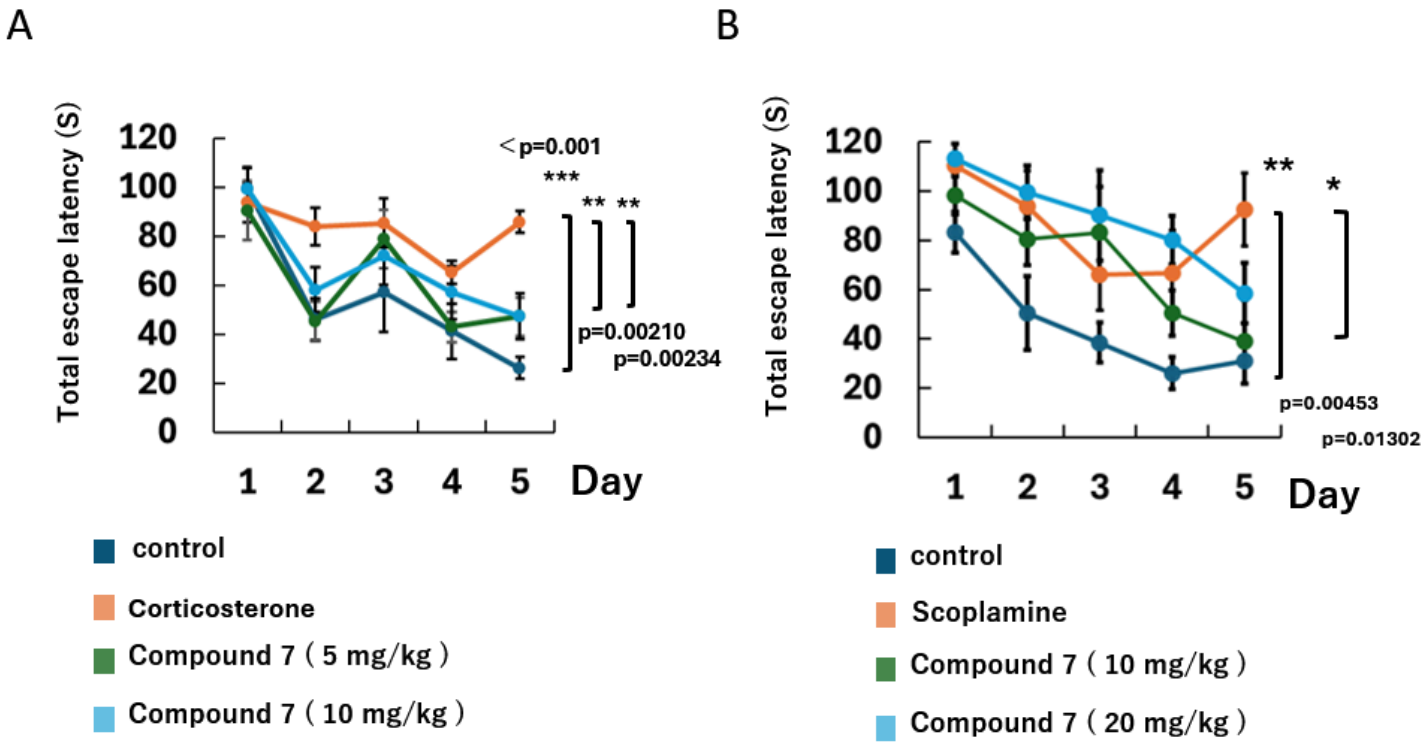

Figure 7

Total escape latency on the barnes maze test. The mice were treated with corticosterone (A) and scopolamine (B). Significance was analyzed using analysis of Dunnett's test ***P<0.001, **P<0.01 and *P<0.05 n=6

Supplementary Files

This is a list of supplementary files associated with this preprint. Click to download.

- Supplementalv32.docx
- image1.png